Coaxial TW Window for Power Couplers and Multipactor Considerations

X. Hanus, A. Mosnier
CEA SACLAY, DSM/DAPNIA/SEA
91191 Gif-sur-Yvette Cedex

Abstract *- A Traveling Wawe coaxial window has been studied for power couplers purposes. The main features, a reduced electrical field in the ceramic and its multipacting free shape are presented. Multipacting simulations results for other window geometries, using a conical or a cylindrical ceramic are also showed.*

1 - Introduction

The principle of Traveling Wave Ceramic, proposed by S. Yu. Kasakov [1], has been examined by different laboratories [2,3] for waveguide-type couplers. We applied this concept to the coaxial-type coupler, envisaged by example for TESLA. In this coaxial TW window, the effective field strength is reduced, pushing away the window breakdown limit. Besides, the TEM propagation mode with no axial Ez component is recovered in the window region, preventing for multipactor phenomena induced by the ceramic disk.

After a review of the principles, HFSS simulations for the final optimization and electron trajectories calculations for multipactor studies are reported. In this study, we focus on electron multipacting which could be induced in the vicinity of coaxial ceramic windows. The conditions that must be satisfied if multipacting involving alumina ceramic is to occur are :

- an electric field component perpendicular to the ceramic must exist
- the secondary emission coefficient δ at the ceramic surface must be larger than unity

The first condition is satisfied in classical "pillbox" arrangements or in the conical window design [4] but not in the coaxial TW window. The second condition is achieved with alumina disks, which have not thin-film coated (such as TiN having a low δ) or when the thin coating is not perfect or has been altered (through electron bombardment or gas adsorption).

2 - TW window principle

The main argument to use such a window is that a pure traveling wave could be established in the ceramic by matching each side of the ceramic disk with capacitive or inductive elements. The equivalent circuit is given fig. 1 where Z is the impedance and L is the distance between the window interface and the axis of the matching element.

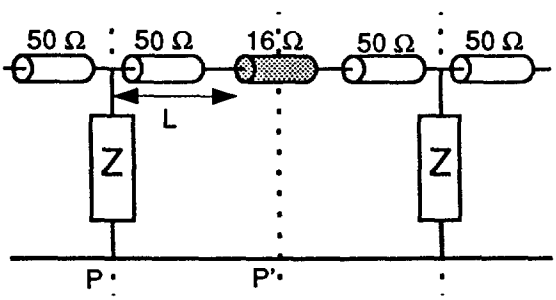

Figure 1 : Equivalent circuit of the matched system

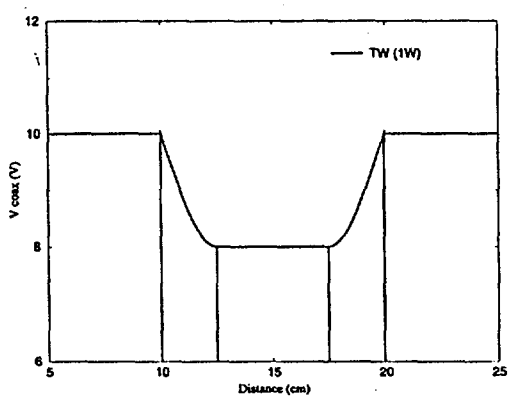

Figure 2 : Voltage along a coaxial guide with a 5 cm thick ceramic and matching irises

The circuit is locally matched for a couple of values (Z, L) which cancels the reflection coefficient at the plane P while a load equal to the impedance of the ceramic line is connected at the plane P'. In that case, the field at the interface and inside the ceramic is lower than for a global matching, where standing waves exist inside the window. Fig. 2 shows the voltage along the guide of such a matched system with an iris as capacitive element. An important feature of this TW system is that the matching is independant of the thickness of the ceramic : one can thus choose a disk sufficiently thick for mechanical rigidity of the coaxial line.

3 - HFSS Simulations

The values of Z and L were first deduced from the equivalent circuit and the final values were determined through HFSS simulations (High Frequency Structure Simulator from Hewlett Packard). A capacitive element (iris) was chosen instead of an inductive one (stub) for fabrication and eventual polarization of the coaxial line reasons. However, in order to keep the field level at a moderate value in the gap of the iris, the impedance of the window was enlarged by doubling its diameter. A lower capacity and hence a larger iris - outer conductor spacing is then obtained, at the expense of a complexity of the fabrication. The final dimensions of the window are given Fig. 3.

The geometry used by HFSS and the computed S_{11} parameter vs. frequency are showed in figures 4 and 5. The results obtained for the optimized TW window are summurized in table 1.

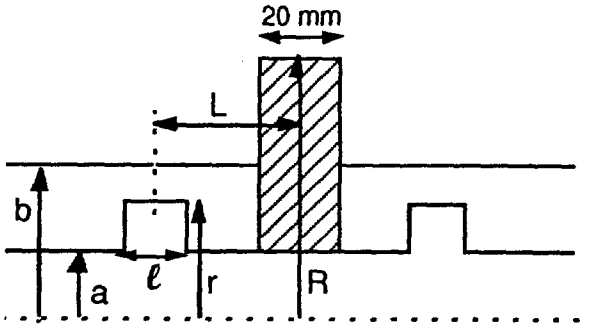

Coaxial guide 50 Ω
inner radius a = 13.385
outer radius b = 30.8
Window (Ɛ =9.8)
Radius R = 71
thickness = 20
Matching iris
radius r = 22.785
length ℓ = 10
Iris/window spacing L = 35.765

Figure 3 : Window geometry used for HFSS simulations (dimensions in mm)

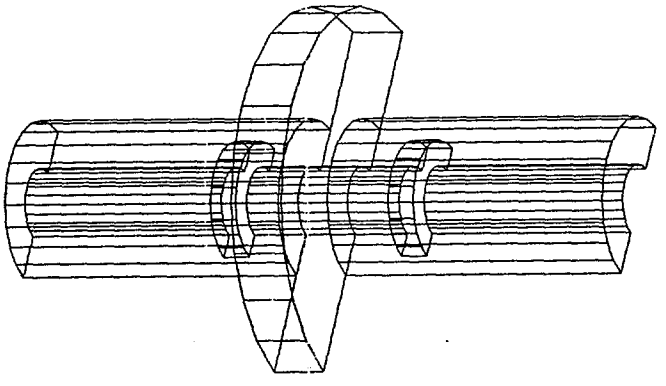

Figure 4 : Geometrical model running on HFSS

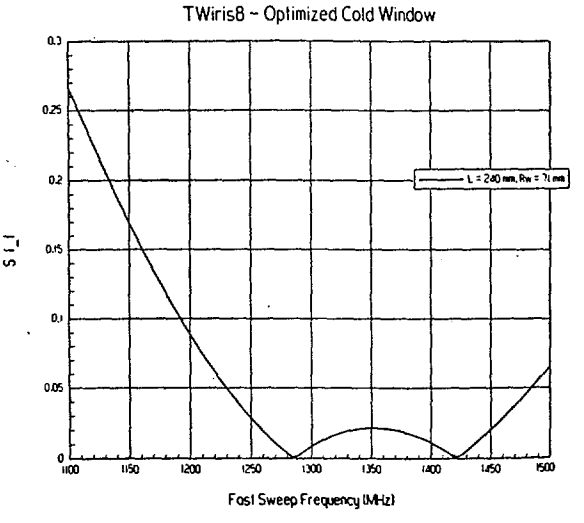

Figure 5 : S_{11} Reflection Bandwidth (MHz)

Reflected power at 1300 MHz	< 0.01 %
E_{max} (iris) / E_{max} (coax)	2.2
Bandwidth (MHz)	[-100; +250]

Table 1

4 - Multipactor Studies in Coaxial Windows

4.1 - Calculation of multipacting electrons

A numerical code computing multipacting trajectories in any axisymmetric structure was developed. It uses the field distributions computed by the cavity code URMEL-T [6]. For coaxial power coupler studies, a resonator is formed by the window itself and a coaxial waveguide at both sides, whose length is adjusted such a way that the correct resonant frequency - 1300 MHz - is found. By changing the boundary conditions (EE or MM), two standing wave field distributions are then computed. A properly matched system gives the same resonant frequency for both boundary conditions [5]. In standing wave mode, the location of the window along the power coupler, at "voltage maximum" or at "voltage minimum", can then be simulated. In traveling wave mode, the time-dependant field is simply obtained by adding both SW fields, but with a 90° phase shift.

The trajectories of electrons were computed using the calculated electric and magnetic fields for three possible configurations : SW at "voltage maximum", SW at "voltage minimum" and TW at last. We restricted this study to multipactor involving the ceramic, because it is the crucial element of a power coupler and can offer a large secondary emission coefficient when the thin coating has been altered. A primary electron is first emitted from the alumina surface, when the local fields drive it towards the vacuum. When the electron impinges a wall (ceramic or copper part), secondary electrons are then emitted if the local fields drive them also outside the wall. Their number is determined by the secondary emission coefficient, which depends on the incident electron's kinetic energy. The total number of re-emitted electrons, if meanwhile no trajectory has been lost, is computed after N impacts either on the alumina or the copper surface. We assumed for the sake of simplicity that the initial kinetic energy of each emitted electron is normal to the surface and is equal to 2 eV. For a complete study, the 3 parameters, the alumina surface, the power and the phase, are successively scanned.

Two coaxial windows were investigated, the conical window [4] and the TW disc window previously described. For the presented simulations, ten equidistant initial emission points on the alumina surface were arbitrary chosen for limiting the computing time, while the RF power and the initial phase were scanned between 2 and 400 kW (step of 2 kW) , and 2 and 360 degrees (step of 2°), respectively.

4.2 - Conical window [4]

In case of standing waves, figure 6 shows the radial electric field along the coaxial guide halfway between both conductors and for both positions of the window, at "voltage maximum" and at "voltage minimum". In the same way but in case of travelling waves, figure 7 shows the modulus of the radial and axial electric field. We note the position of the ceramic at the center of the plots. While no relevant multipacting trajectories were found on the upstream side of the ceramic, strong and stable multipactor phenomenon broke out on the downstream side of the ceramic. Multipactor of order 1 involving ceramic and outer conductor and multipactor of order 4 involving ceramic solely could be disclosed. The figures 8 (in the transverse plane) and 9 (in the plane r - time in rf periods) give an example of radial multipacting trajectories moving back and forth at the same position of the conical window.

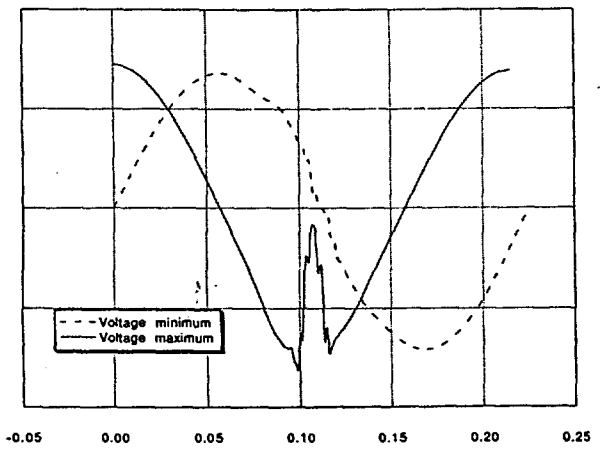

Figure 6 : Standing Wave Er field

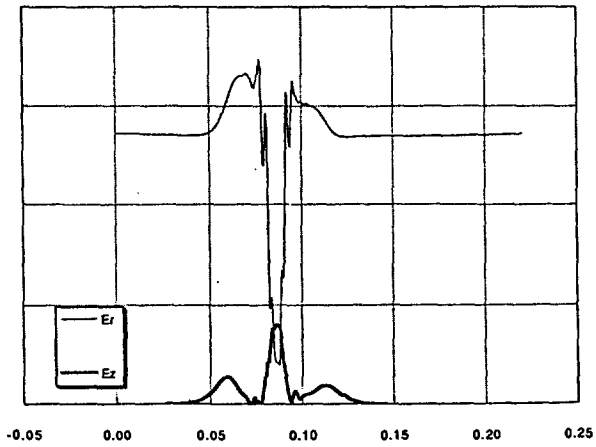

Figure 7 : Traveling Wave Er and Ez fields

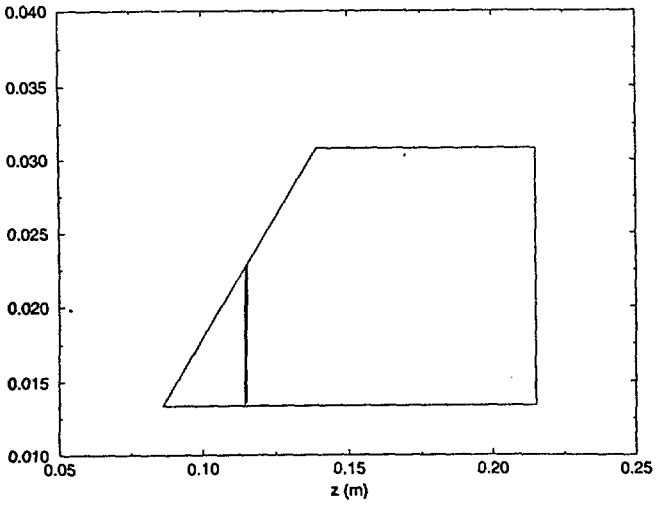

Figure 8 : Multipactor order 4 involving ceramic (transverse plane)

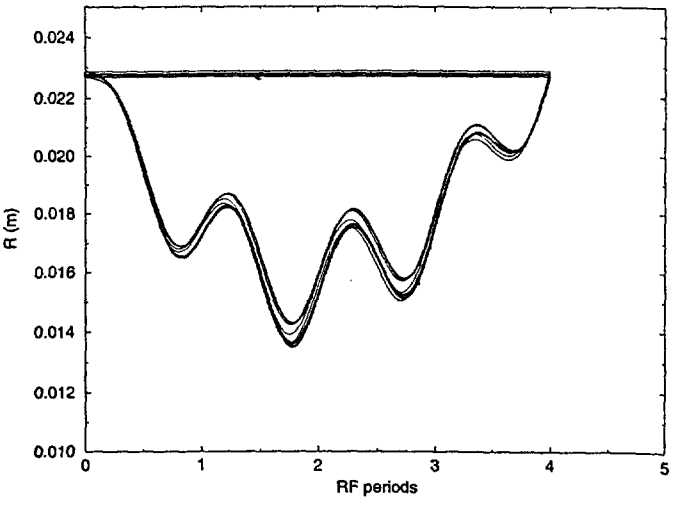

Figure 9 : Multipactor order 4 involving ceramic (plane r - time in rf periods)

Scanning simultaneously the ceramic surface, the power and the starting rf phases, we can get an idea of the width and of the strength of the multipactor for a given window. For example for standing waves mode, figure 10 shows the total number of emitted particles after 20 impacts for the downstream side of the conical window, located at "voltage maximum". The standard curves of secondary emission coefficients vs. impacting energy for copper and alumina without coating were used in the simulations. For travelling waves mode (figure 11), multipacting trajectories were also found, but at higher incident power (> 250 kw) and with a smaller strength.

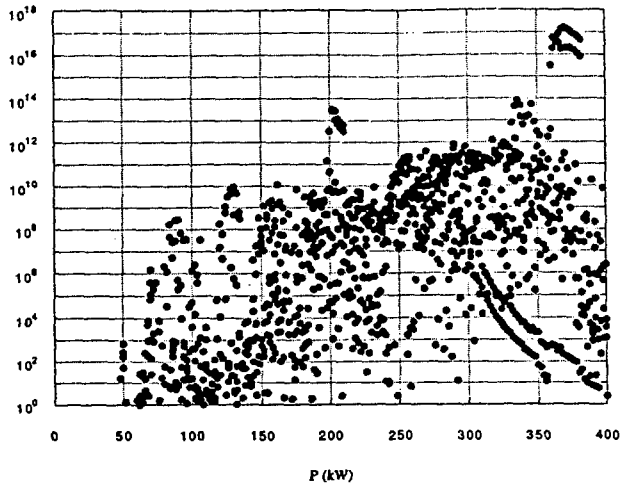

Figure 10 : Conical window (downstream side) at "voltage maximum"

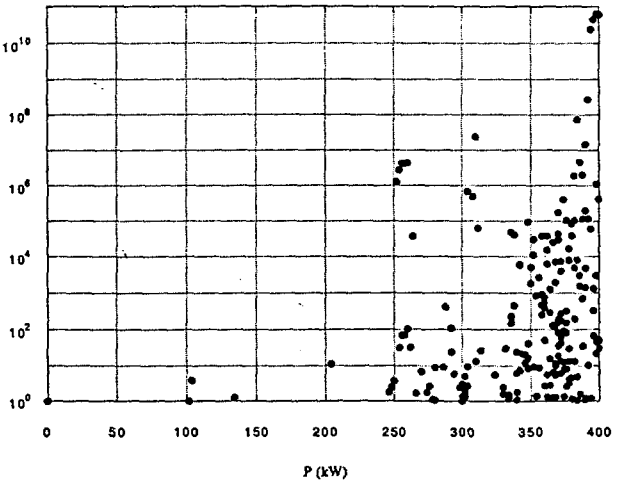

Figure 11 : Conical window (downstream side) travelling waves mode

4.3 - Travelling Wave Window

Figure 12 shows the electric field plot for the coaxial TW window, located at "voltage maximum", computed by Urmel-T. We note that the axial field vanishes near the ceramic surface. For all standing waves and travelling waves simulations, we didn't find any multipactor involving the ceramic, as expected. Starting from the ceramic surface, multipacting trajectories can occur at high incident power (> 350 kw) but only between the inner and outer copper conductors. Such trajectories are shown on figure 13 and are harmless for the alumina disk.

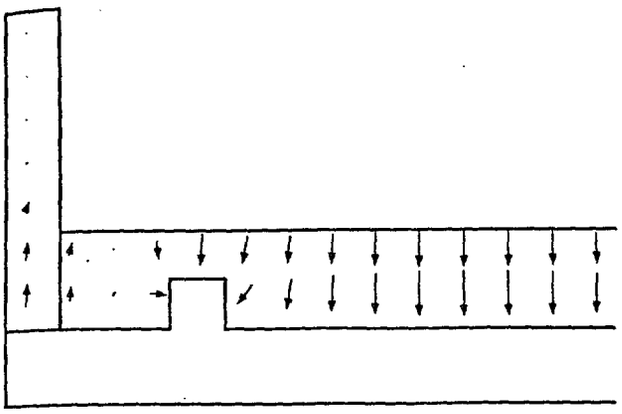

Figure 12 : Electric field plot of the TW window at "voltage maximum"

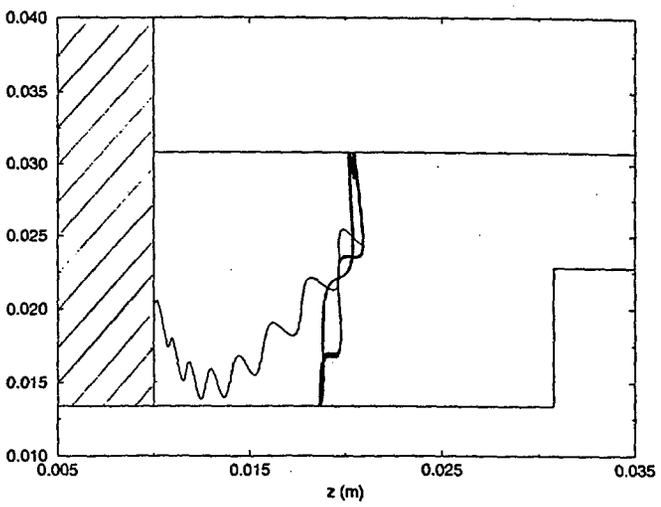

Figure 13 : Multipacting trajectories in the TW window w/o ceramic bombardment

References

[1] Yu. Kasakov, "Increased Power RF-Window", *BINP Preprint 92-2*, Protvino, 1992

[2] S. Michizono, Y. Saito, H. Mizuno and S. Yu. Kasakov, "High-power Test of Pill-Box and TW-in-Ceramic Type S-Band RF Wndows", *KEK Preprint 94-157*, Tsukuba, Dec. 1994

[3] N.M. Kroll et al., "Design of Traveling Wave Windows for the PEP-II Coupling Network", *SLAC-PUB-95-6901*, May 1995

[4] M. Champion et al., *Proc. of the 1993 Part. Acc. Conf.*, Washington, pp 809-811

[5] S. Yamaguchi, Y. Saito, S. Anami and S. Michizono, "Trajectory Simulations of Multipactoring Electrons in an S-Band Pillbox RF Window", *IEEE Trans. On Nucl. Sci.*, 39 (2), pp. 278-282, April 1992

[6] T. Weiland, *Nucl. Inst. and Meth.*, 216, 1983